8351

p35

NASA Technical Memorandum 101667

Dynamic and Control Assessment of the Space Station Freedom Payload Pointing System

(NASA-TM-101667) DYNAMIC AND CONTROL ASSESSMENT OF THE SPACE STATION FREEDOM PAYLOAD POINTING SYSTEM (NASA) 35 p N91-21225
CSCL 22B
Unclas
G3/18 0008351

David T. Shannon, Jr.

February 1991

NASA
National Aeronautics and
Space Administration

Langley Research Center
Hampton, Virginia 23665-5225

DYNAMIC AND CONTROL ASSESSMENT OF THE SPACE STATION FREEDOM PAYLOAD POINTING SYSTEM

Abstract

An analysis of the proposed Space Station Freedom Payload Pointing System (PPS) was performed to assess its dynamic payload pointing capability in the dynamic environment of the Space Station Freedom (SSF). In addition, the stability and control of the Space Station Freedom was examined to verify the capability of its control devices to accommodate the impact of PPS operations. An analysis of the PPS ability to provide continuous, accurate pointing was performed and compared to the program requirements specified in the 1988 Program Definition and Requirements Document (PDRD). Results indicated that the PPS was not able to perform within the program requirements during the worst case scenario of a shuttle hard docking maneuver to the port side SSF docking adapter. The PPS maintained marginal pointing accuracy during crew treadmill activity. The Space Station attitude control system easily accommodated all PPS operations simulated. The PPS caused a negligible impact on Freedom's controls environment.

Introduction

Figure 1 represents the baseline Space Station Freedom (SSF) configuration at the time this analysis was performed. The SSF provides a permanently manned research facility in low-earth orbit. The current design includes four pressurized modules, eight photovoltaic solar arrays mounted on a truss structure called the "transverse boom", which is 500 ft in length, and an active cooling system which uses radiators. The nominal orbit of this station will be about 220 nautical miles. SSF orientation will be local vertical/local horizontal (LVLH) with an orbital inclination of 28.5 degrees. Freedom's attitude will be controlled by multiple Control Moment Gyros (CMGs) managed by a linear quadratic regulator feedback control law.

A Payload Pointing System that would accommodate different classes of payloads has been considered for development by the Space Station Freedom program. This study made an assessment of the dynamics and control of this Space Station device. This paper will describe the PPS and its operation, discuss the procedures used to analyze the system and show results of the analysis.

The PPS analysis was done to determine if the device could operate within the specifications set in the 1988 Program Definition Requirements Document (PDRD), especially in the presence of a major disturbance like a shuttle orbiter hard-docking. In order to determine the PPS and SSF interactions, it was necessary to understand the effect of each on the control environment of the other. In addition, it was necessary to determine the effects of the various PPS components on each other such as interaction between the Station Structural Interface Adapter (SIA) and the Payload Interface Adapter (PIA). These two PPS components enable the connection of the pointing apparatus to the SSF truss and provide the interface for the payload. (See Figure 2) The remainder of the paper describes the PPS and the SSF/PPS interface analysis.

Description of the PPS

The PPS dynamic mechanism elements are displayed in Figure 2. The Yoke is the main component of the PPS and provides most of the structural support for the payload in this configuration. The Cross Elevation Ring is the component that rotates about the Y-axis of the PPS and provides the pitch control for the payload. The Azimuth drive enables the rotation of the payload about the Z-axis and is attached to both the Yoke and the PIA. The PIA provides the interface of the payload pointing element with the Structural Interface Adapter (SIA). This SIA in turn provides support for the pointing device and is fixed to the truss of the SSF.

Two types of configurations for double and triple axis Payload Pointing Systems were studied; the CG-mount and the End-mount as shown in Figure 3. Various gimbal sizes, which were payload specific were surveyed for pointing performance. However, the flexibility of the Cross Elevation Ring had the most significant impact on the performance with the gimbal size being a secondary consideration. Thus, the model of the PPS which was chosen for this study was that which was most acceptable in terms of cross elevation, flexibility and gimbal performance. That model was the two-axis CG-mount system which accommodated the largest prescribed payload was chosen for analysis.

In discussing the PPS and the SSF interaction, it is necessary to note that their coordinate systems initially are parallel. See Figure 1. The selected PPS configuration has two degrees of freedom, about the Y and Z axes. Rotation about the Y-axis is provided by the Yoke along the line where the Cross Elevation Ring is attached parallel to the Y-axis of the SSF. The point at which the PPS Y-axis intersects the Yoke-Cross Elevation Ring junction is referred to as joint A. (refer to Figure 4.) The PPS Z-axis of rotation is parallel to the Z-axis of the SSF and is located in the middle of the Yoke base. The Azimuth Drive and the PIA rotate about this axis and the junction where these two components were connected is referred to in Figure 4 as joint B.

The types of payloads that the PPS is designed to accommodate are those requiring a CG-mount with a maximum mass of 6,000 kilograms and a maximum height of 12 meters. The PPS is intended to allow continuous pointing at celestial bodies by using an inertial tracking controls system which damps out disturbances. This network of adapters and components enables the system to provide a broad viewing range and an accurate pointing capability under steady state conditions.

The PPS operational requirements are as follows:

o	Performance Requirements	arc sec (3 sigma)
	- Jitter (over 1 sec)	10
	- Knowledge	36
	- Accuracy	60
	- Stability (over 1800 sec)	30
o	Slew rate: 1 degree/second from terrestrial	

2 degree/second from celestial

- o Minimum Gimbal Frequency: 10 Hz
  - lower frequencies cause control problems
  - goal : 20 Hz
- o Maximum Torque: 9 Nm
- o Payload Capacity:
  - Inertia - 20,000 kgm**2
  - length - 12 m
  - diameter - 4 m

The control system used in this study is an inertial sun tracking system based on a Proportional Integrated Differential/Lag controller with a bandwidth of about 0.6 Hz. This type of controller is also proposed for other SSF articular parts such as the photovoltaic arrays. Figure 5 shows a block diagram of the control system. The apparent rate of the target being tracked by the PPS is assumed to be known a priori and this knowledge is used for feed-forward purposes. This control law factors in the torques and forces generated by disturbance profiles, PPS and SSF motions, the CMG control torques and the pointing error which is the difference between the actual position and the desired position. It then compiles this information and sends an output signal to the motor that prompts it to make necessary corrections to the pointing. The function of the control law is to null the pointing error.

Analysis Procedures

The research was performed using an integrated multidisciplinary engineering analysis capability called IDEAS**2. It was necessary to determine the dynamic behavior of the SSF structure both before and after the PPS was attached to it in order to assess the impact of PPS operations on the station. For this purpose, an equivalent beam finite element model of the SSF and the PPS was created (See Figure 6). Using this method, the struts of each bay of truss were substituted with a beam element with the equivalent stiffness of the bay and the total mass lumped at the nodes. For this type of model a normal mode analysis for the lower modes is more accurate than for the higher modes. Next, a normal mode dynamic analysis was performed first on the SSF alone and then on the station with the PPS attached to the top of the transverse boom, two bays to the port side of the geometric center. Modes 7 through 22 were the only natural modes studied because the first 6 modes are rigid body modes and the modes higher than the 22nd were highly distorted due to model limitations. The results of this analysis indicated that the addition of the PPS to the top of the SSF had a negligible impact on the natural modes and frequencies of the station.

To determine the effect of PPS operations on the rigid body controllability of the Space Station, a 120 degree elevation angle slewing maneuver at 2 degrees per second was simulated. Results showed that the SSF attitude control system easily accommodated the PPS induced disturbances.

Further analysis was performed to determine if the PPS could operate within specifications during a shuttle hard dock to Freedom, which is the largest dynamic disturbance anticipated. This is a particularly important issue because scientists ideally desire continuous pointing for their experiments at all times. However, systems integration engineers felt that it would not be feasible to design the PPS with the ability to perform within the documented requirements during major disturbances. The forcing function shown in Figure 7 models the force of the shuttle docking that was applied to the SSF at the port side docking adapter. A rigid body analysis of the SSF was adequate to determine those forces transmitted to the PPS due to the impact of the shuttle docking maneuver. The response of this maneuver was sensed at joints A and B on the PPS, the locations of the control system motors. These results were analyzed using a fast Fourier transformation to determine the dominant frequency and the PPS control system's ability to operate within its specifications.

An additional flexible body analysis was performed using a less severe transient disturbance forcing function. The forcing function shown in Figure 8 is a model of the force caused by crew treadmill activity at the aft node of the habitat module. The responses of this disturbance were sensed at joints A and B.

A rigid body analysis was performed,whereby the SSF articular parts were allowed to move and the PPS tracked the sun. This analysis determined the reaction torques the PPS control device had to produce to provide continuous accurate tracking. The results of this analysis are discussed below.

Results

The analysis described determined that the attachment of the PPS on the SSF at the proposed location caused a negligible effect on the modal behavior of the SSF. This can be seen in the normal mode dynamics analysis plotted in Figure 9 which shows an insignificant change in the lower natural frequencies of the SSF with the PPS attached. The slight differences, manifested in modes 12 through 22, are caused by the fact that these modes were more sensitive to the additional mass than the lower frequency modes.

The previously mentioned simulated slewing maneuver was performed to identify the operational impacts of a dynamic PPS on the SSF. The results of this analysis demonstrated that the SSF is capable of controlling disturbances caused by PPS operations. Figure 10 shows that the PPS simulated slewing maneuver using the maximum allowable payload, produced a perturbing torque of 15.7 Nm. This graph shows that the maneuver was started at a 60 degree orbit angle slewing the payload at 2 degrees per second. In the first case the PPS was fixed and the second case the PPS was slewed 120 degrees. The SSF's CMG's are able to supply 270 Nm of control torque each, thus the PPS disturbances were well within the capability of the SSF control devices.

The results of the analyses showed that the PPS could not perform within 4 operational requirements. The result of the forced response analysis displayed in Figure 11 shows that the PPS did not meet the jitter requirement following the orbiter hard dock. A fast Fourier transformation was performed on the angular displacement data to determine the frequency of the dominant mode. The dominant frequency as labeled in Figure 12, corresponded to mode 8, the transverse boom bending mode. Observation of the mode shapes showed that the location of the PPS, as indicated in Figure 13, is near a nodal point for mode 8. These findings indicated that other positions may need to be examined as possible locations for the PPS.

When simulating a sun-tracking payload, analysis showed that the 9 Nm motor proposed for this task was not sufficient for the PPS to generate the necessary controlling torques to counteract the torques induced by the disturbances. Figures 14 through 21 show the forces and torques transmitted to the two joints of the PPS where the control motors are located. Figure 14 depicts the forces sensed at joint A while Figure 15 shows the torque. Figure 16 shows the forces affecting joint B and Figure 17 shows the torques. The 200 Nm torque caused by the shuttle impact transmitted to joint A significantly exceeded the control authority of the PPS.

The perturbing forces and torques generated by crew treadmill activity were also studied. The results presented in Figures 18 through 21 show that only one component of the torques impacting joint A approached the capabilities of the proposed PPS. Figure 18 shows the force transmitted to the PPS joint A. Figure 19 shows the transmitted torque. Figure 20 shows the crew activity induced force transmitted to joint B. The torque caused by crew treadmill activity is shown in Figure 21. The reaction torques experienced at joint B were well within the controlling capabilities of the PPS control device. This analysis revealed that the PPS was marginally capable of performing within the system requirements during crew treadmill activity.

Conclusion

Both rigid and flexible body analyses were performed on the proposed SSF Payload Pointing System. A systems control analysis was also performed . The results showed that some significant modifications need to be made in order for the proposed PPS to function within specified pointing requirements during a shuttle hard dock maneuver. Since this docking event is not a frequent occurrence, the requirement for pointing during such a period probably should be dropped or relaxed. It was concluded that the PPS operations have little effect on the Space Station Freedom control capability.

References

1. Hughes, R., "Conceptual design of Pointing Control Systems for Space Station Gimbaled Payloads," Paper 86-1986-CP, AIAA GNC Conference, Williamsburg, VA., Aug. 18-20, 1986.
2. Laskin, R., et. al., "Space Science/Space Station Attached Payload Pointing Accommodation Study -- Pointing Performance Analysis White Paper," JPL Publication D-5249, January, 1988.
3. "Code E Space Station Pointer System Study-Study Team Final Report", Jet Propulsion Laboratory, Jan 1988.
4. Class, B.F., Smagala, T.J., Welch, R.V., "Space Station Payload Pointing System(PPS) Final Report " Fairchild Space Company, December 1986.
5. Smagala, T.J. and McGlew, D., "CETF Space Station Payload Pointing System Design and Feasibility Study," Paper AAS 88-041, AAS GNC Conference, Keystone, CO., Jan 30-Feb 3, 1988.
6. Hammesfahr, A, "The Spacelab Instrument Pointing System Performance Operations," AIAA Paper 85-6073-CP, Shuttle Environment and Operation II Meeting, Houston, TX., Nov. 1985.
7. NASA Space Station Freedom Program Level II Systems Engineering and Integration Assembly Sequence CR BB000468 Supporting Data, Document SSE-E-88-R20, Sept. 1988.

8. NASA Program Definition Requirement Document (PDRD) 1988

9. Mission Requirement Data Base Document GE/TRW BR-02, June 1986

10. Swales and Associates, Inc. 84-035 Technical Report on the PPS 11/27/87

SPACE STATION CONFIGURATION

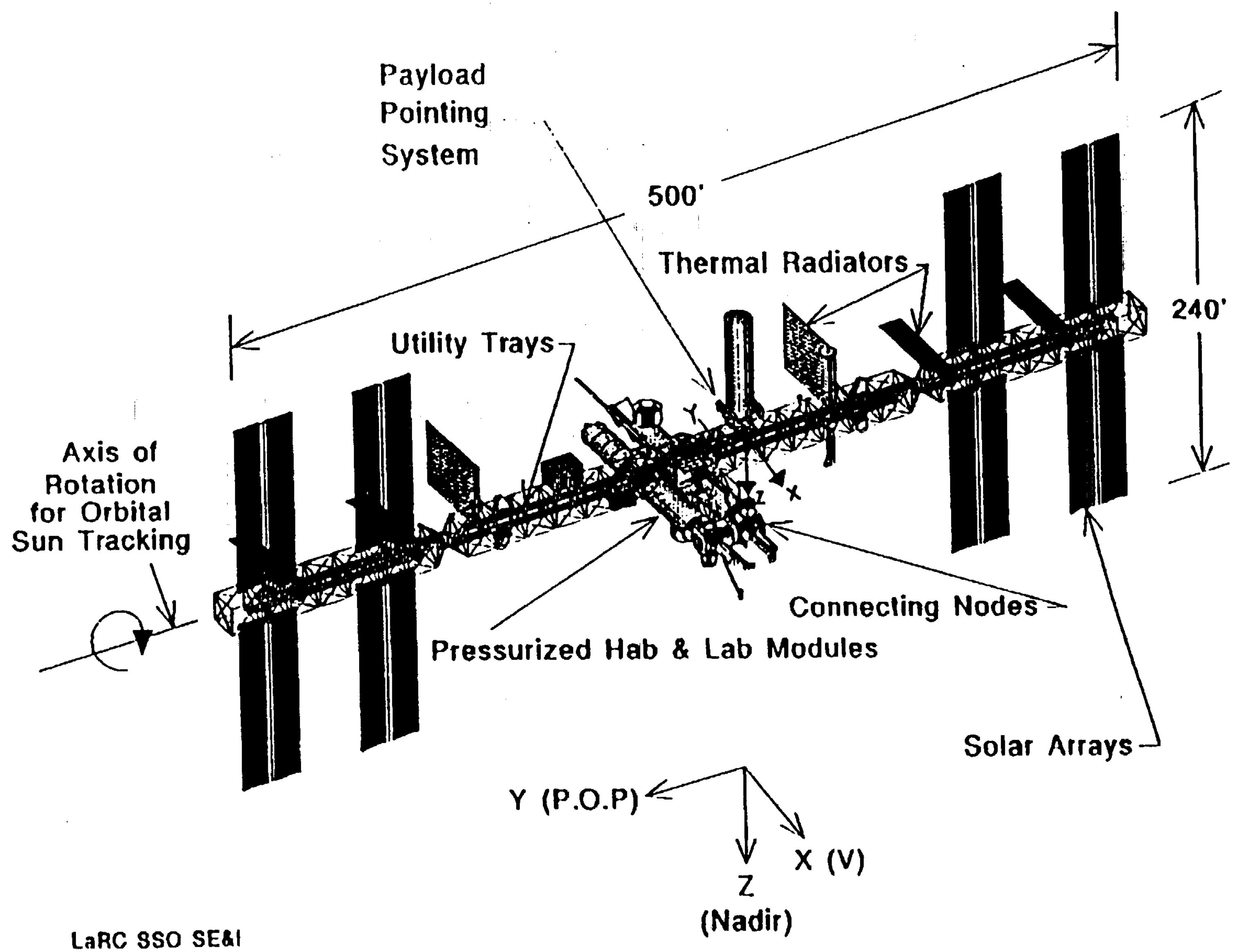

Figure 1

PPS DYNAMIC MECHANISM MODEL

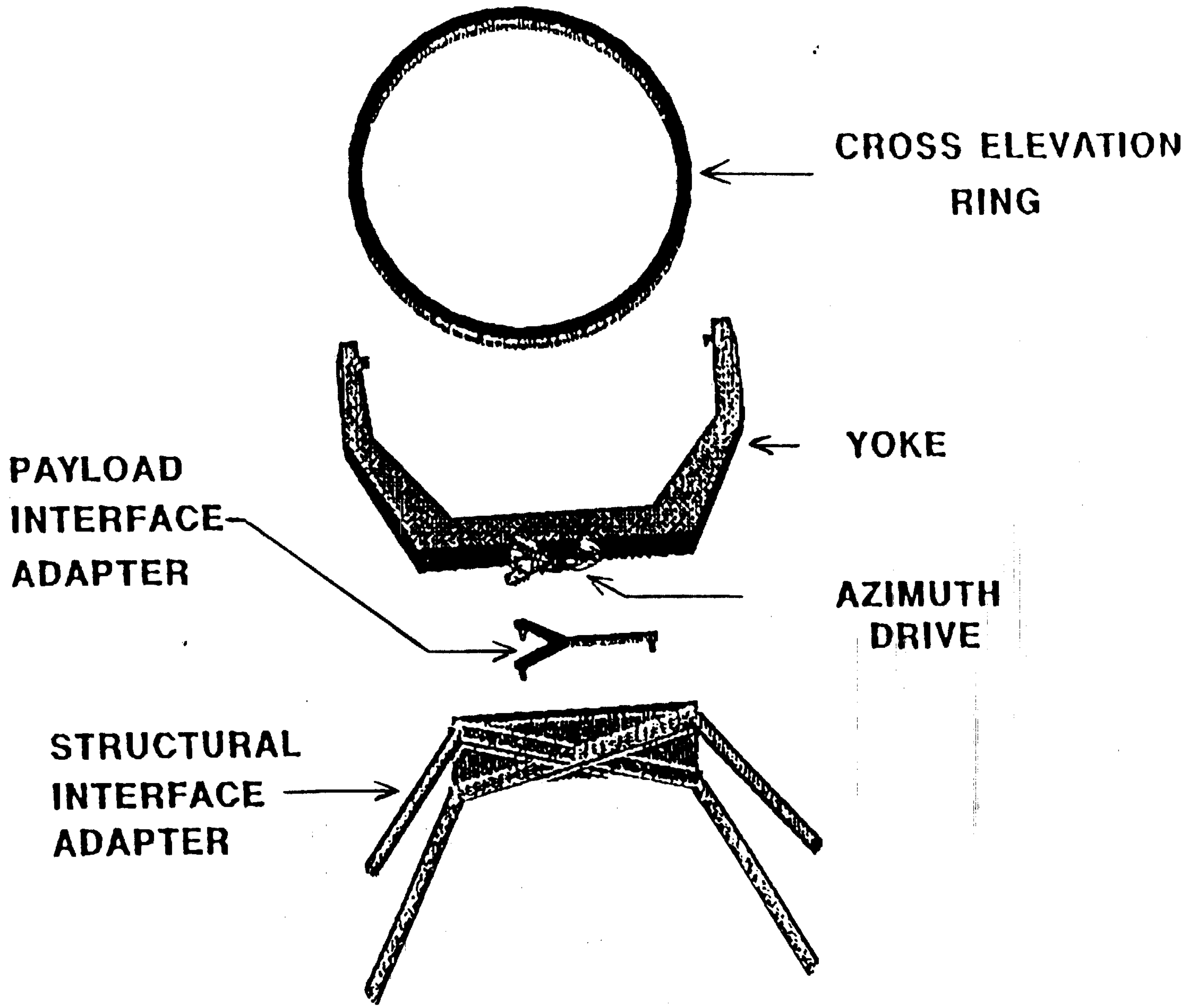

LaRC SSO SE&I

Figure 2

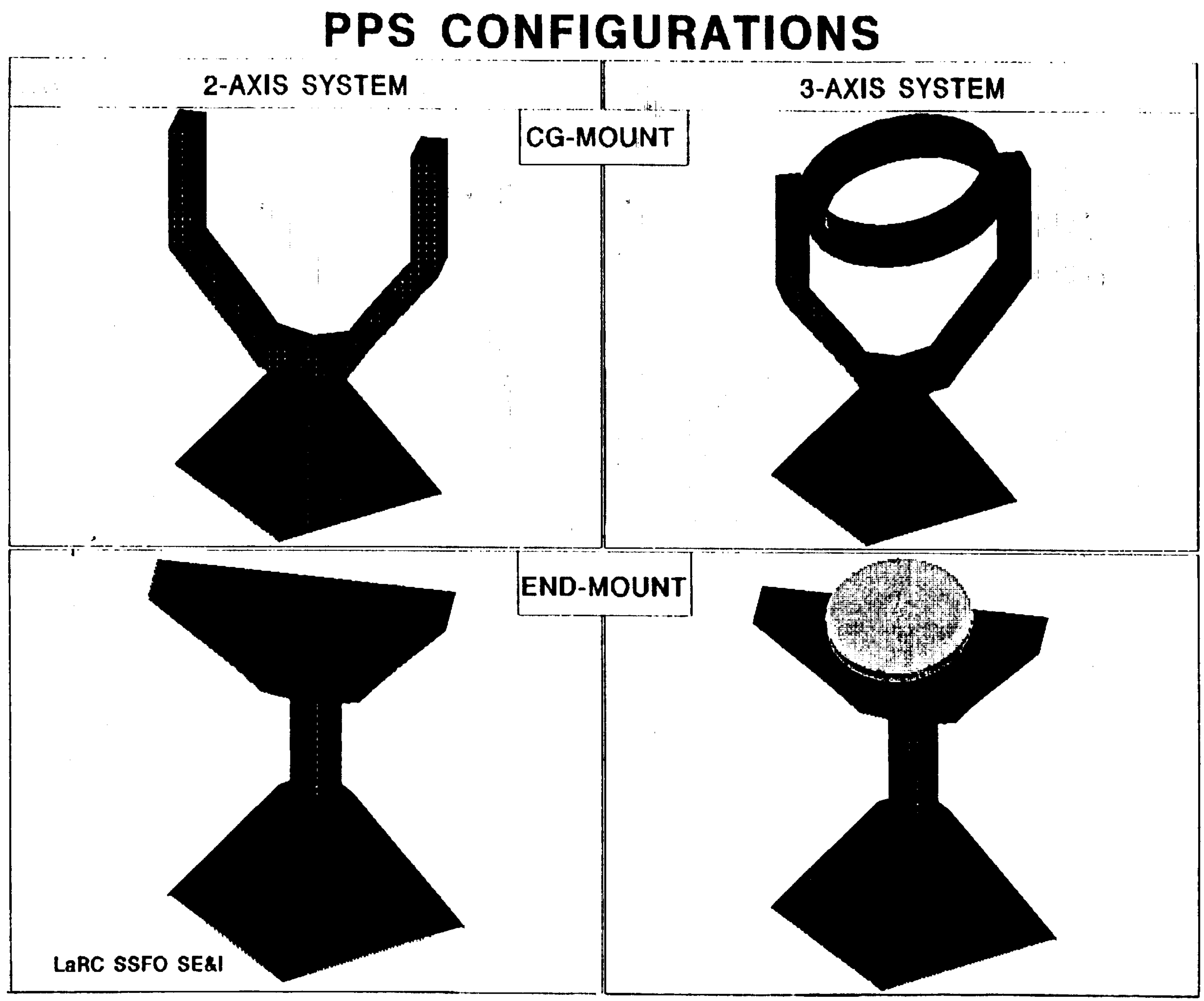
PPS CONFIGURATIONS
2-AXIS SYSTEM
3-AXIS SYSTEM
CG-MOUNT
END-MOUNT
LaRC SSFO SE&I

Figure 3

THE PAYLOAD POINTING SYSTEM

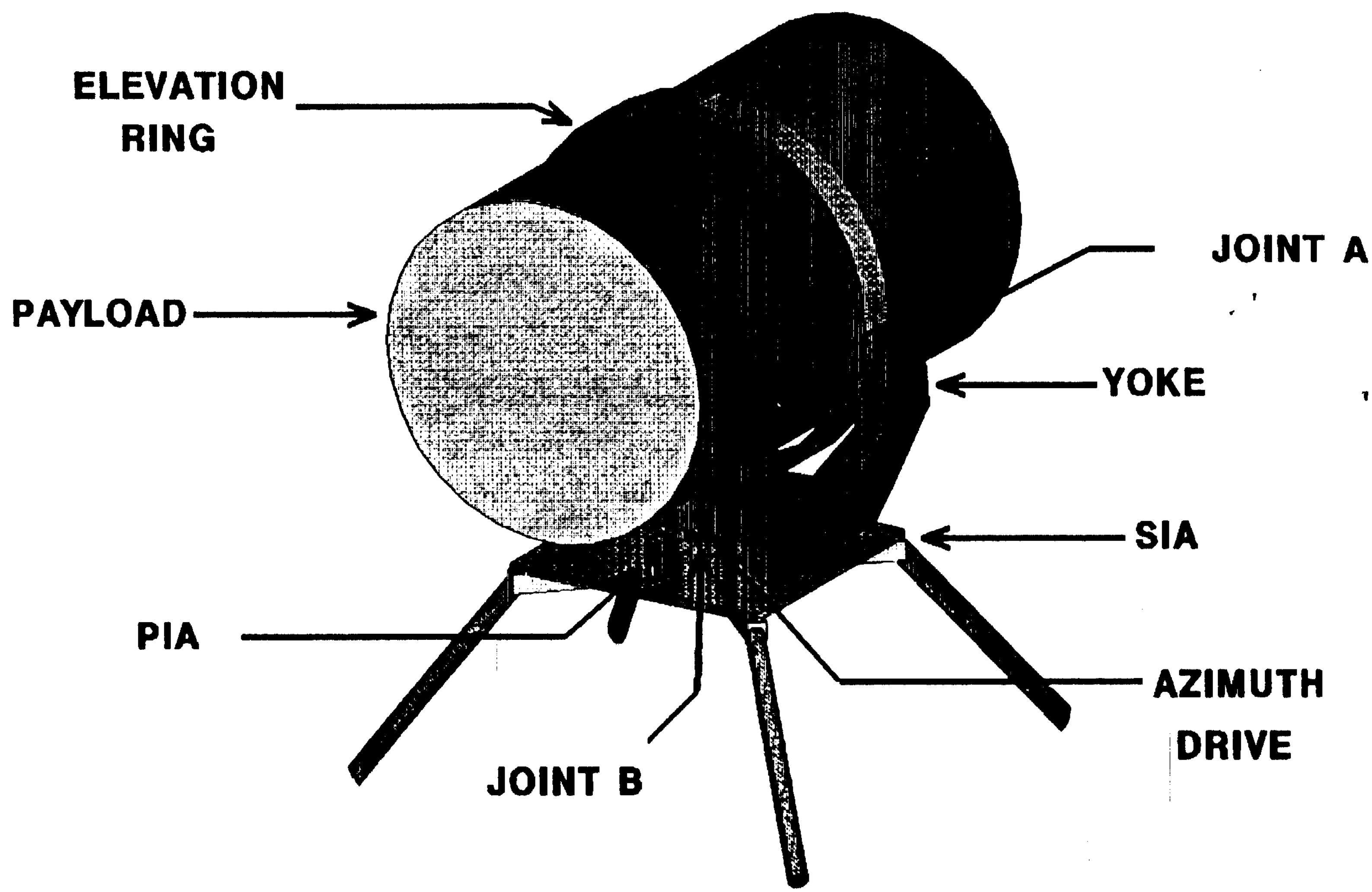

LaRC SSFO SE&I

Figure 4

CONTROL SYSTEM DYNAMIC BLOCK DIAGRAM

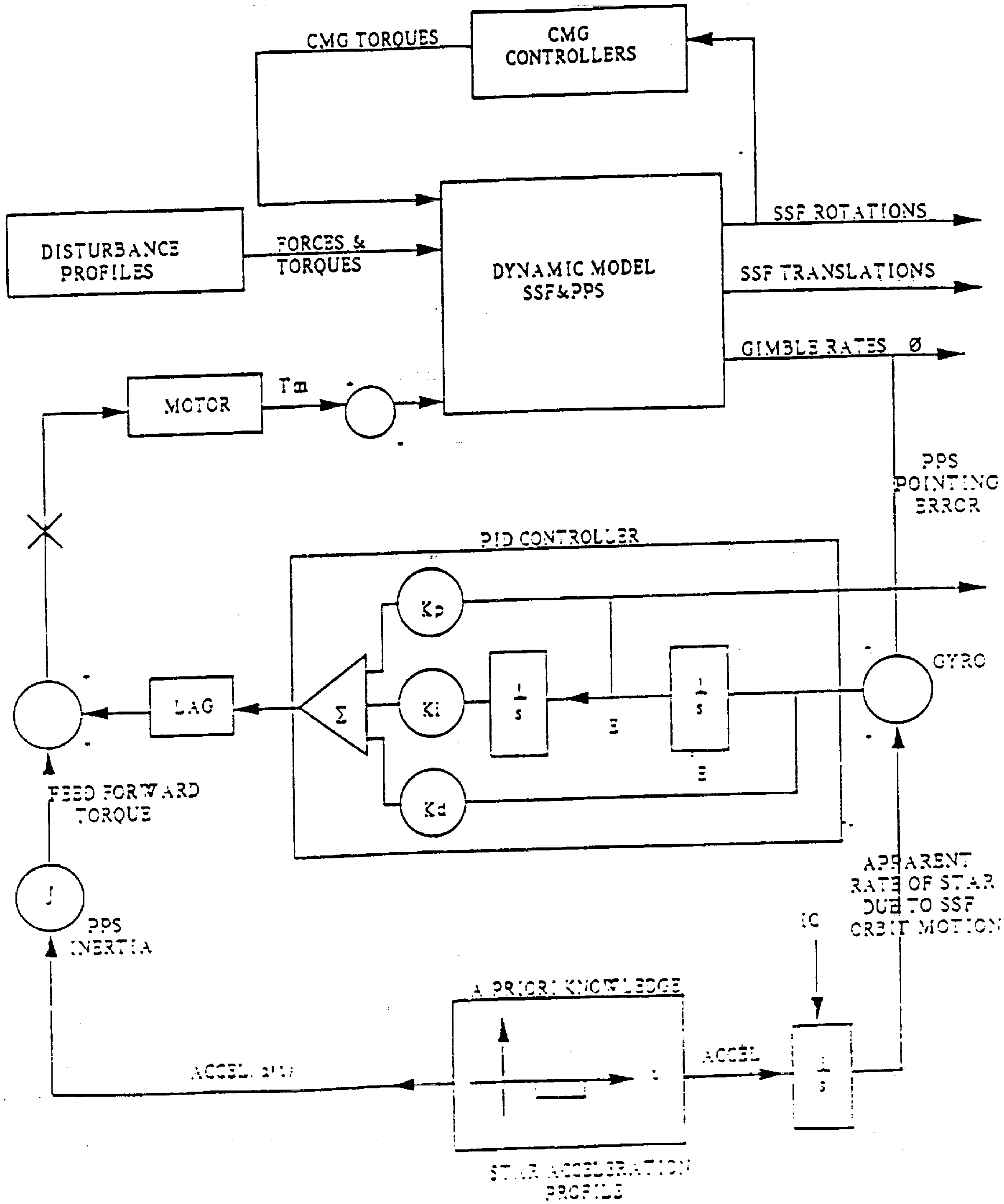

Figure 5

ANALOGOUS BEAM FINITE ELEMENT MODEL

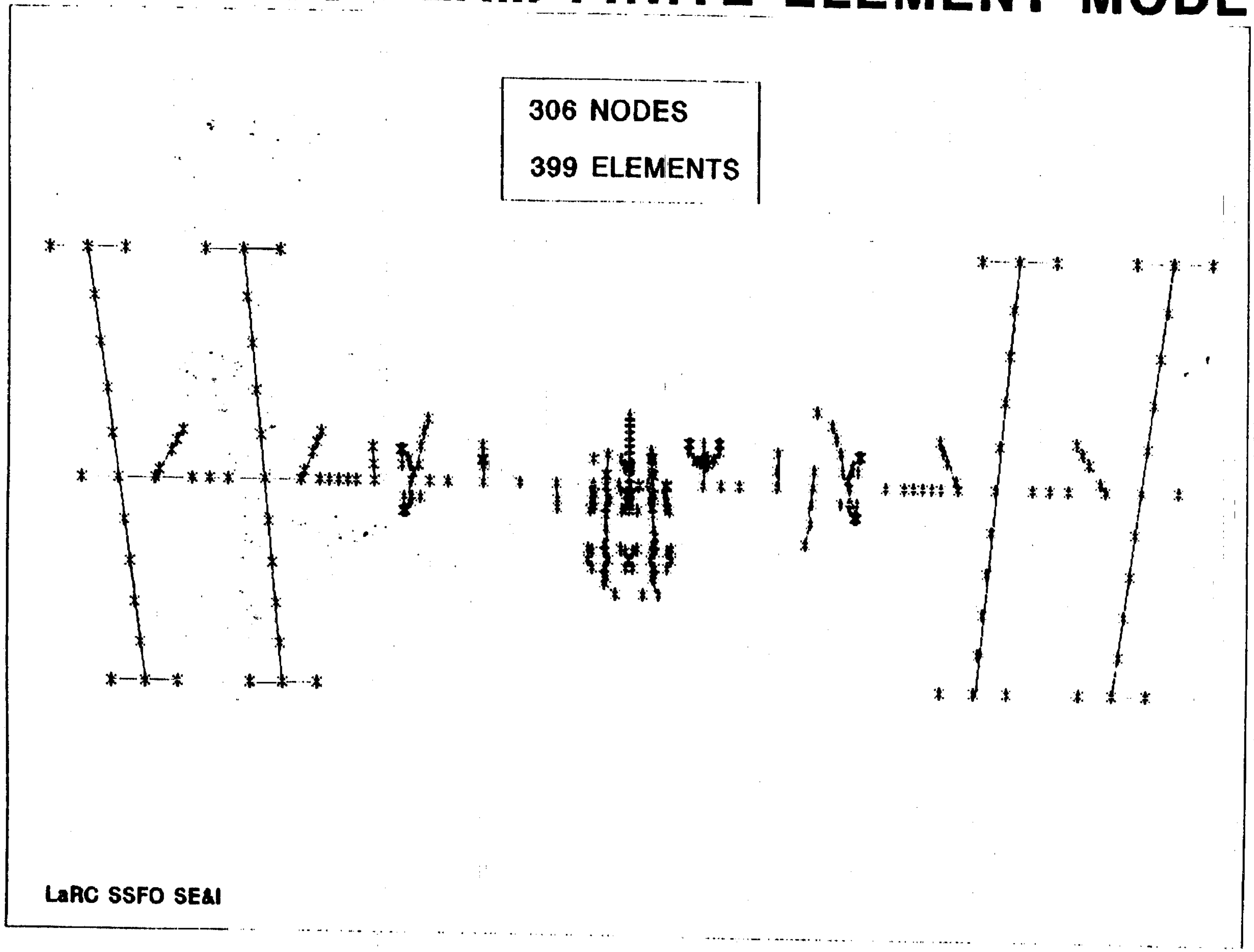

Figure 6

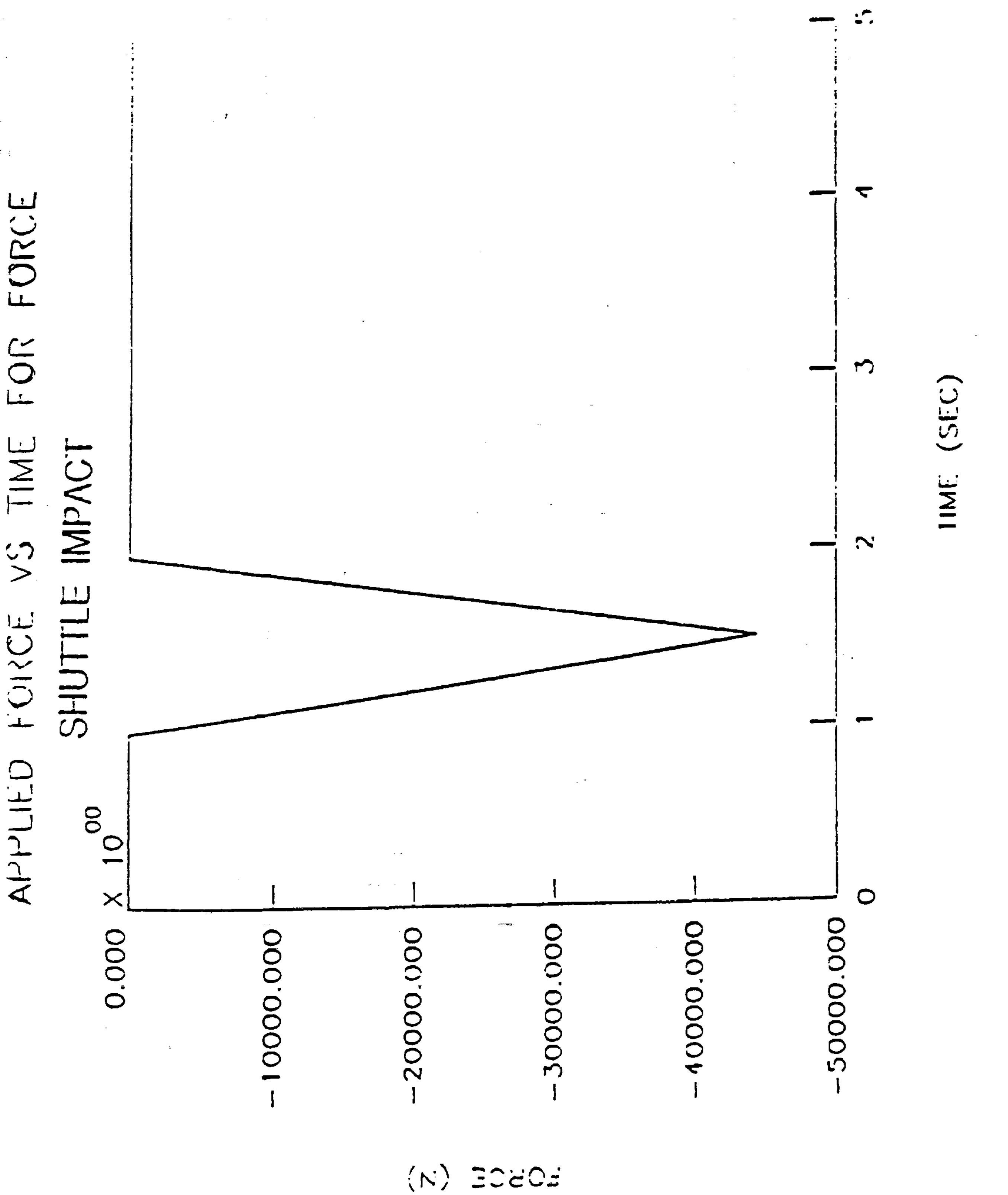
APPLIED FORCE VS TIME FOR FORCE
SHUTTLE IMPACT
x 10^00
0.000
-10000.000
-20000.000
-30000.000
-40000.000
-50000.000
FORCE (N)
0
1
2
3
4
TIME (SEC)

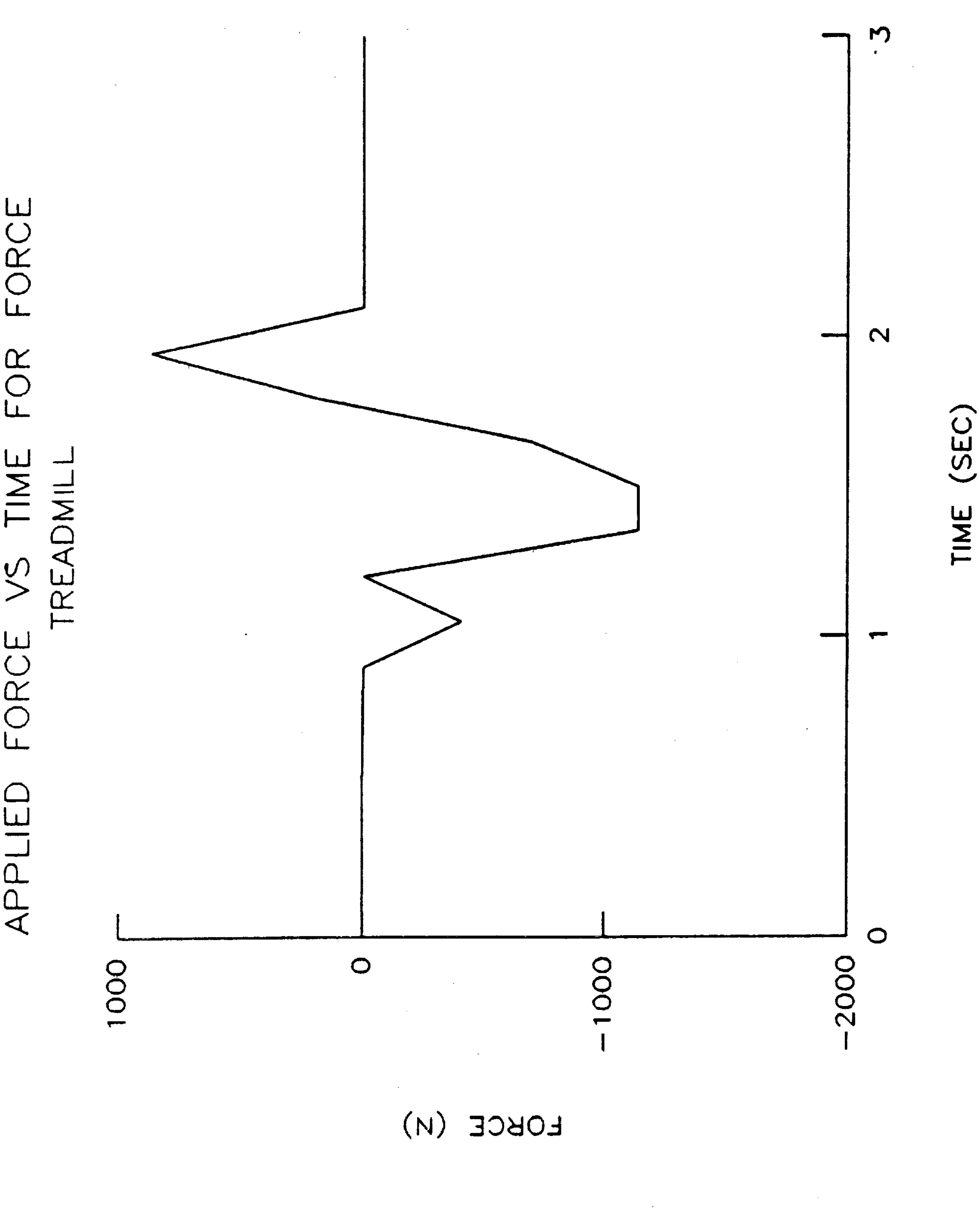
APPLIED FORCE VS TIME FOR FORCE
TREADMILL
1000
0
−1000
−2000
FORCE (N)
0
1
2
3
TIME (SEC)

Figure 8

NATURAL MODES AND FREQUENCIES

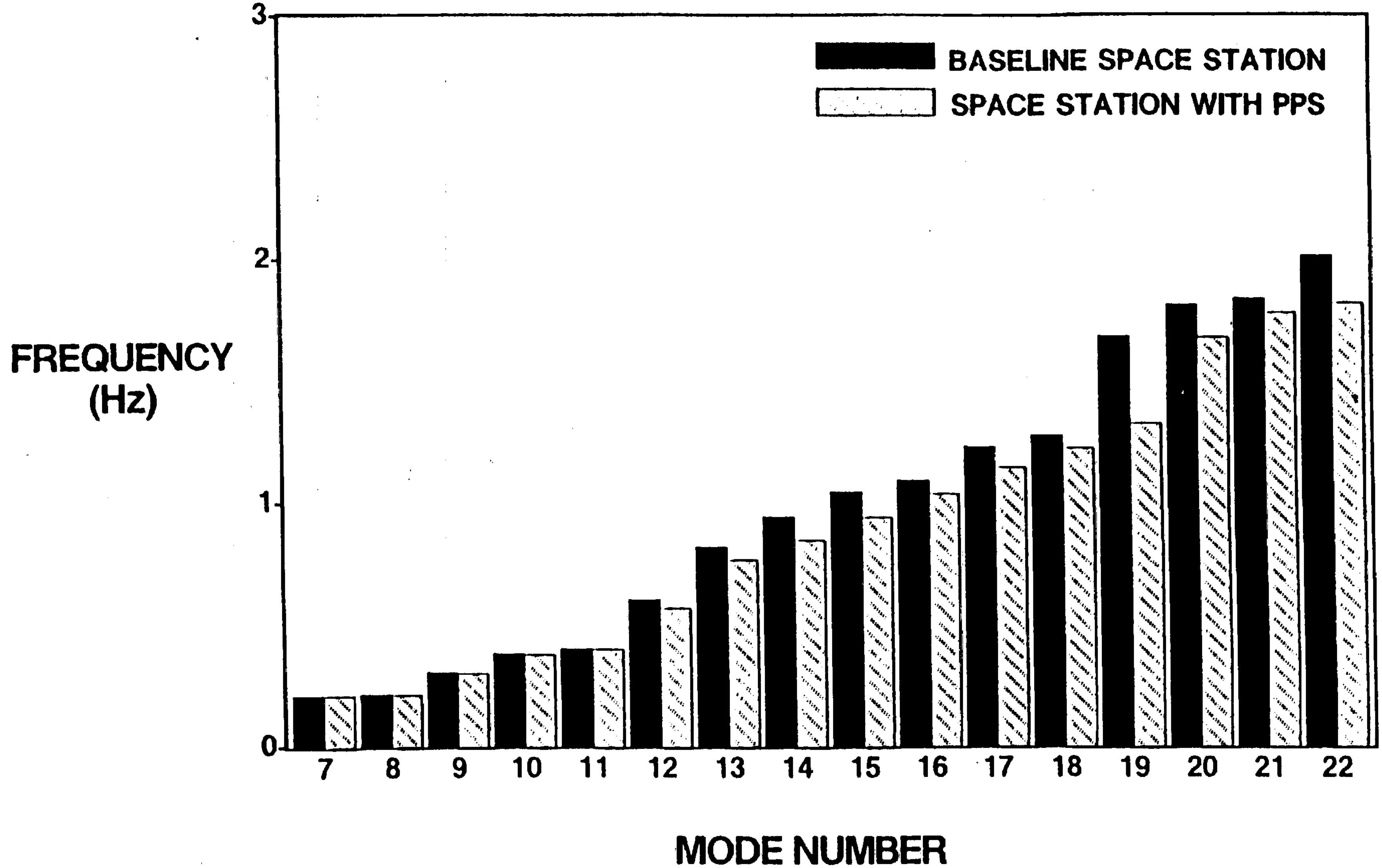

Figure 9

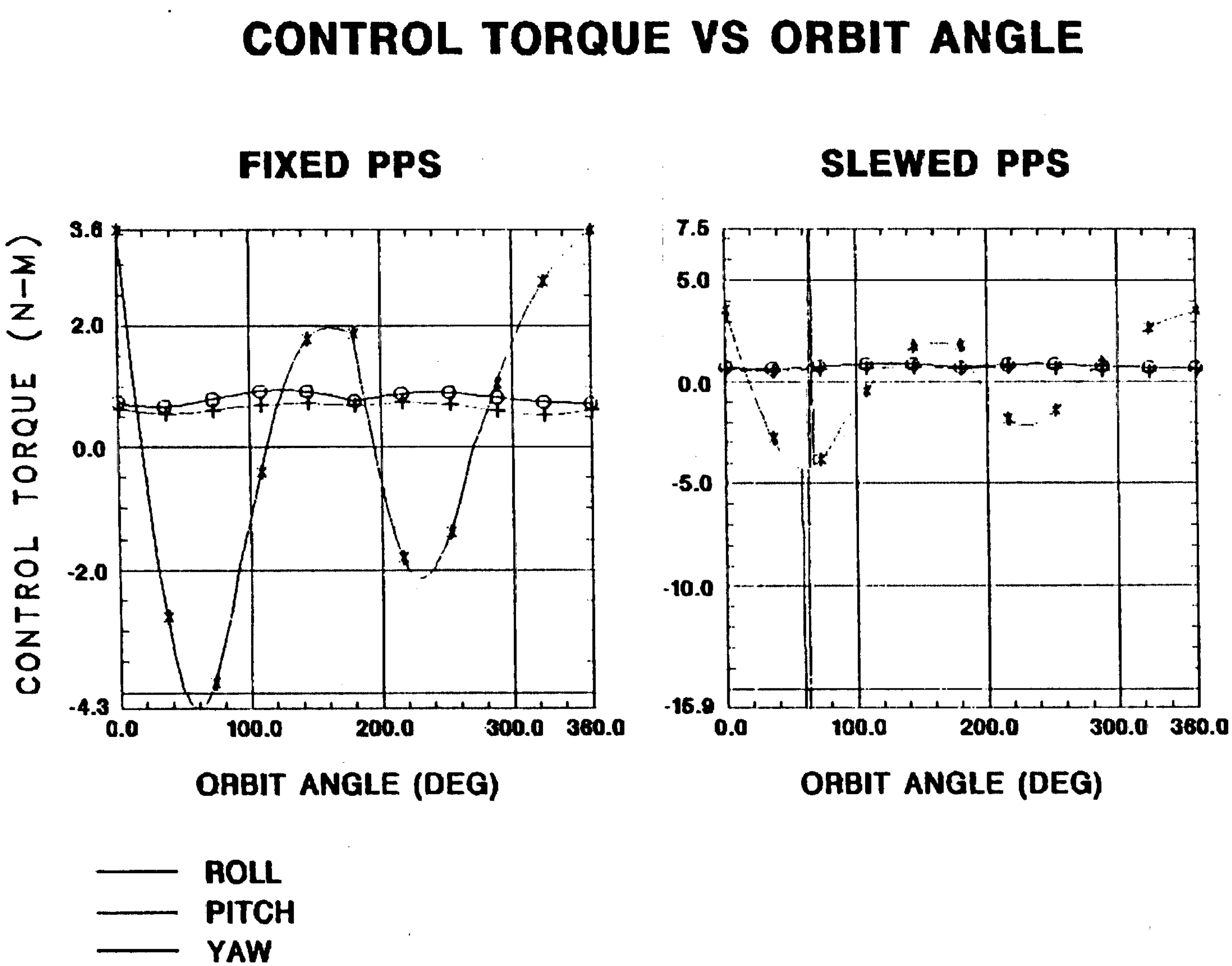
CONTROL TORQUE VS ORBIT ANGLE
FIXED PPS
SLEWED PPS
CONTROL TORQUE (N-M)
3.6
2.0
0.0
-2.0
-4.3
7.5
5.0
0.0
-5.0
-10.0
-15.9
0.0
100.0
200.0
300.0
360.0
ORBIT ANGLE (DEG)
ROLL
PITCH
YAW

Figure 10

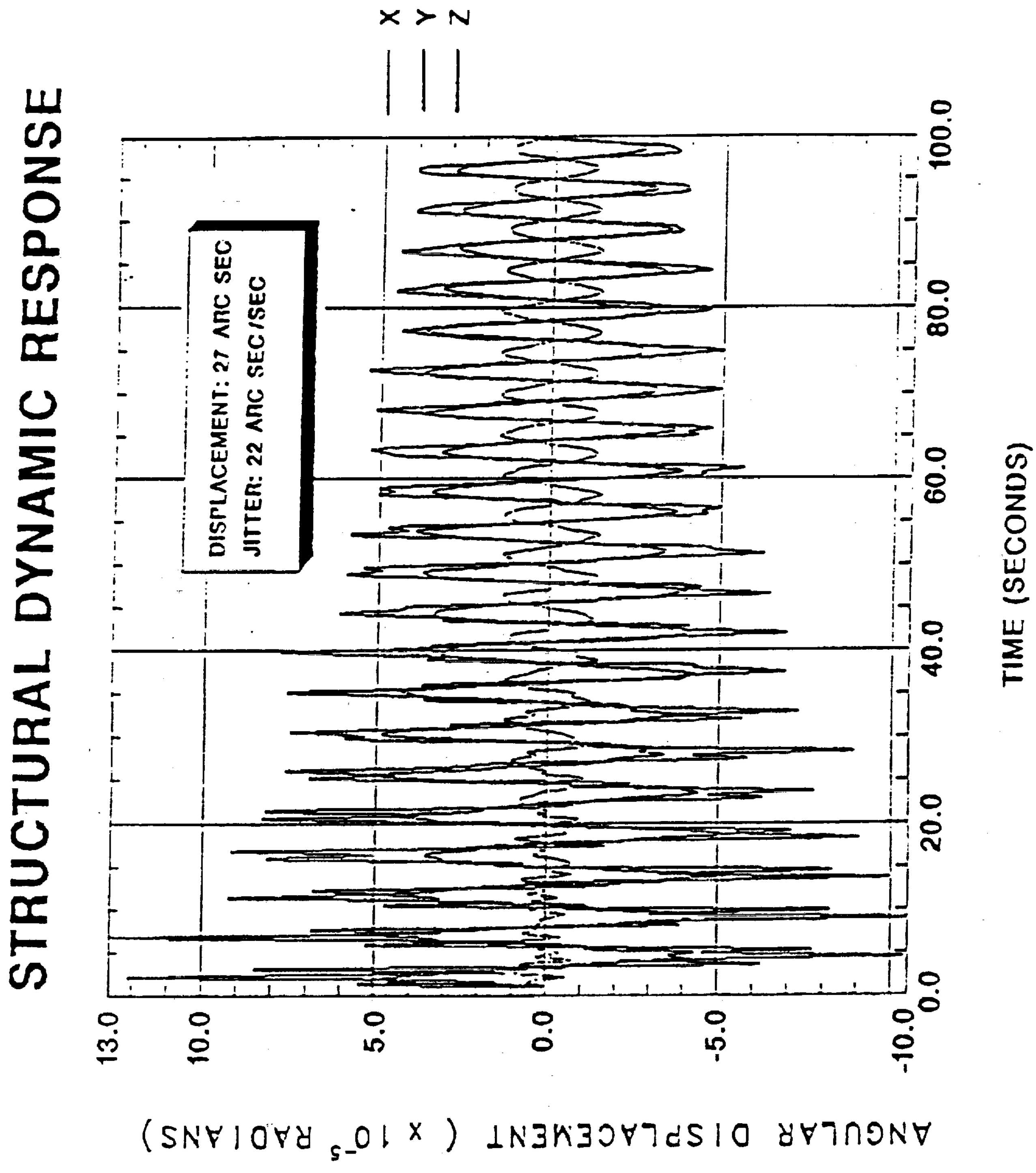
STRUCTURAL DYNAMIC RESPONSE
X
Y
Z
DISPLACEMENT: 27 ARC SEC
JITTER: 22 ARC SEC/SEC
13.0
10.0
5.0
0.0
-5.0
-10.0
0.0
20.0
40.0
60.0
80.0
100.0
TIME (SECONDS)
ANGULAR DISPLACEMENT (x 10^-5 RADIANS)

Figure 11

FOURIER TRANSFORM USED TO LOCATE DOMINANT MODE

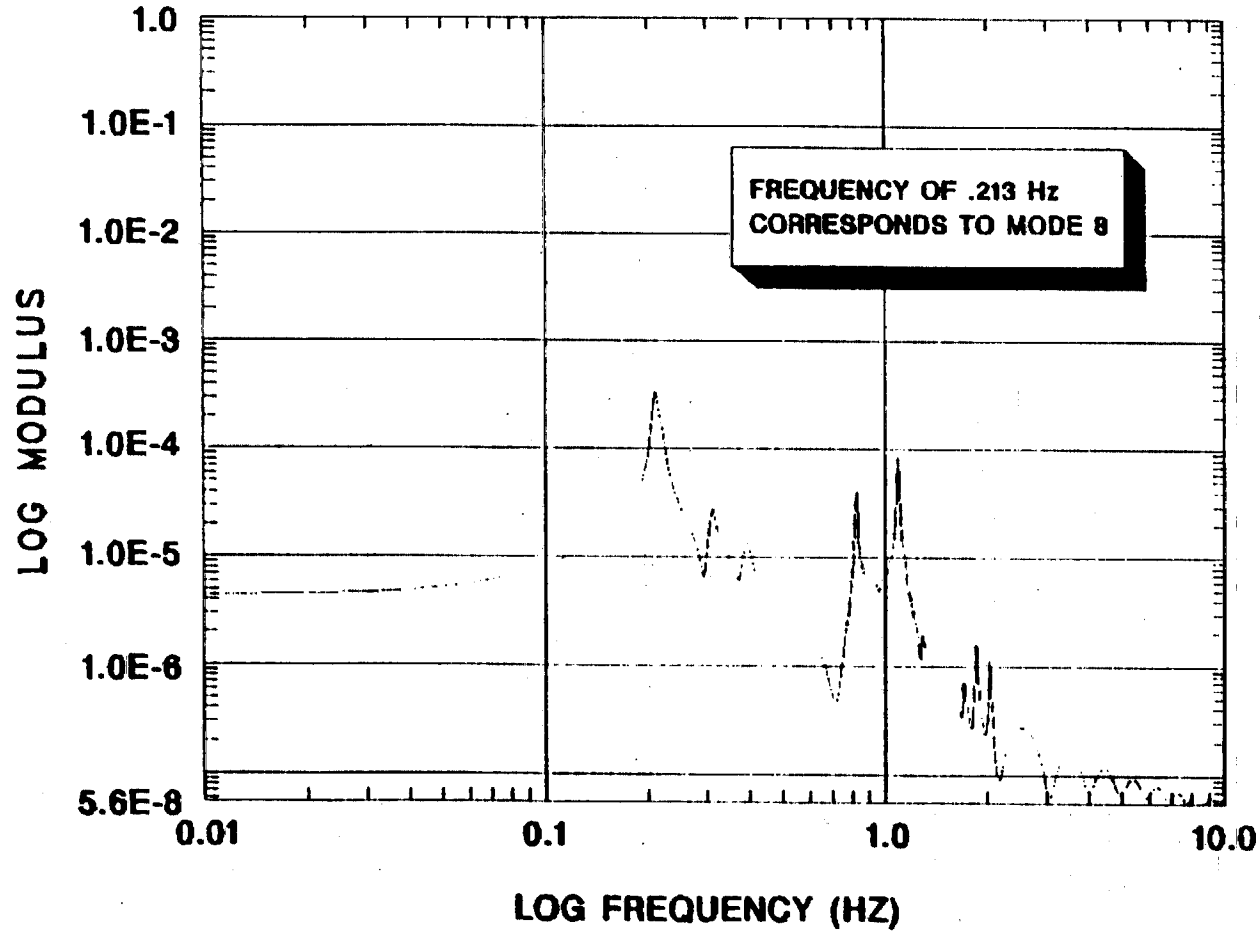

Figure 12

DOMINANT FREQUENCY MODE

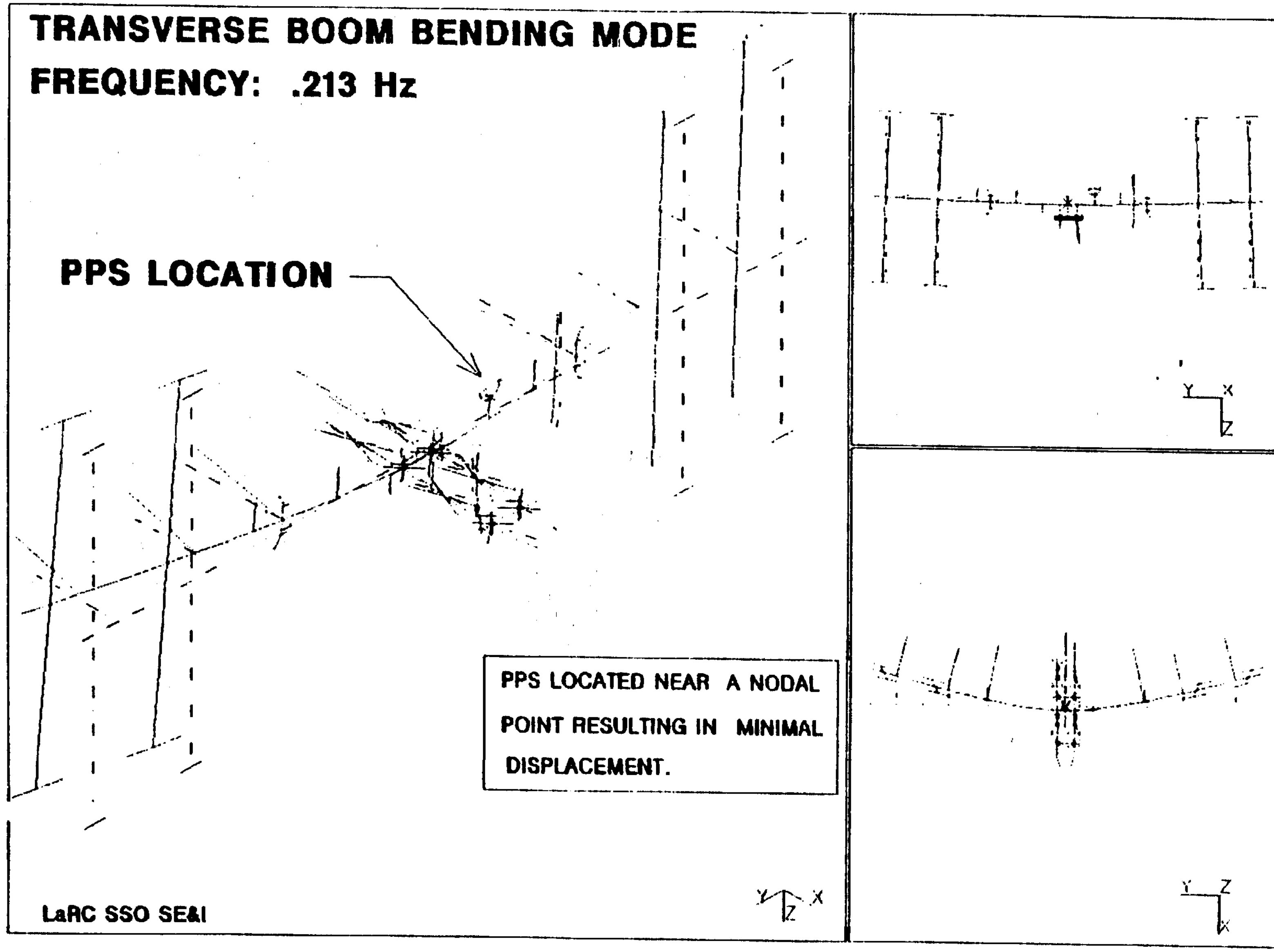

Figure 13

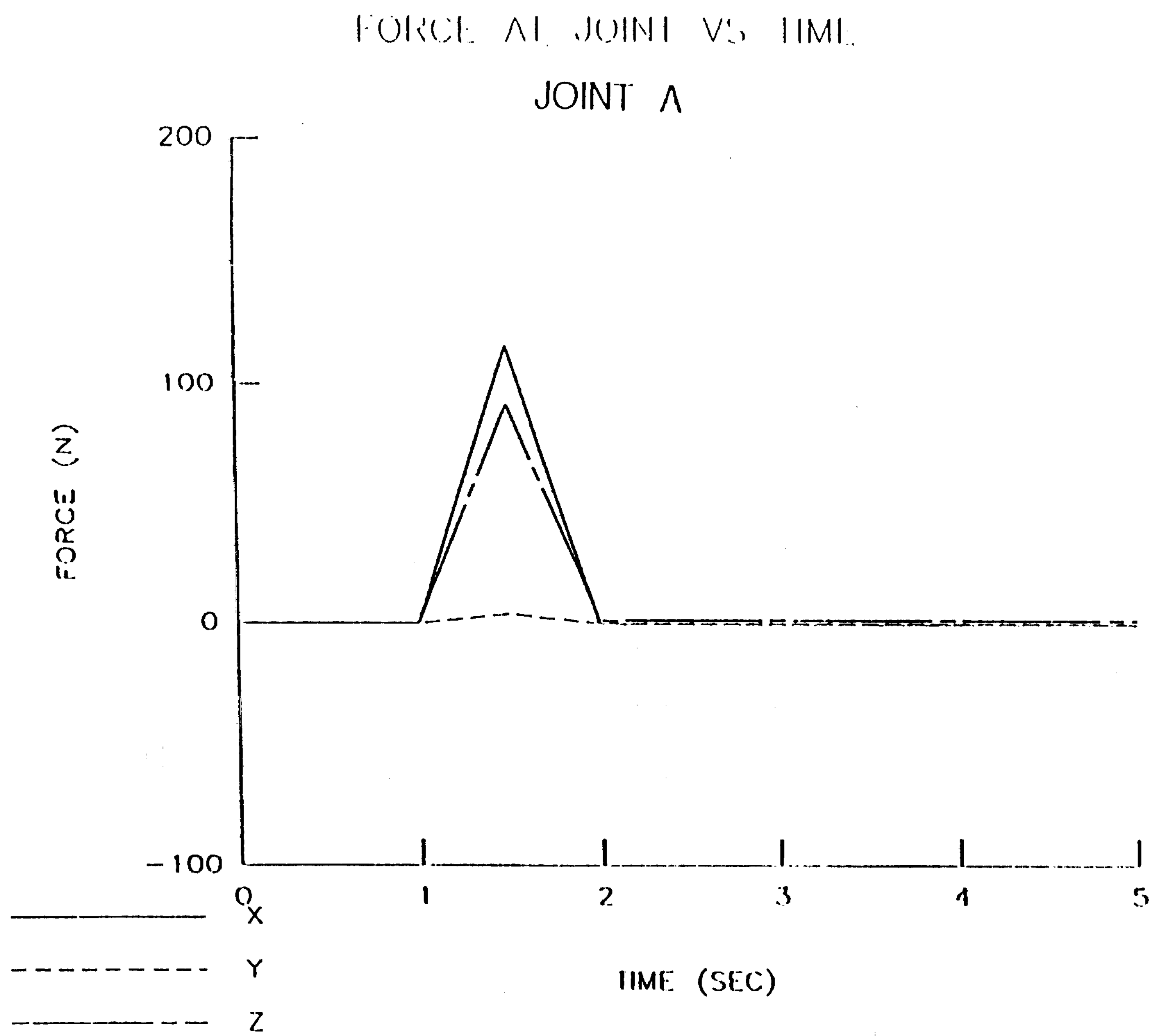
FORCE AT JOINT VS TIME
JOINT A
200
100
0
-100
FORCE (N)
0
1
2
3
4
5
TIME (SEC)
X
Y
Z

Figure 14

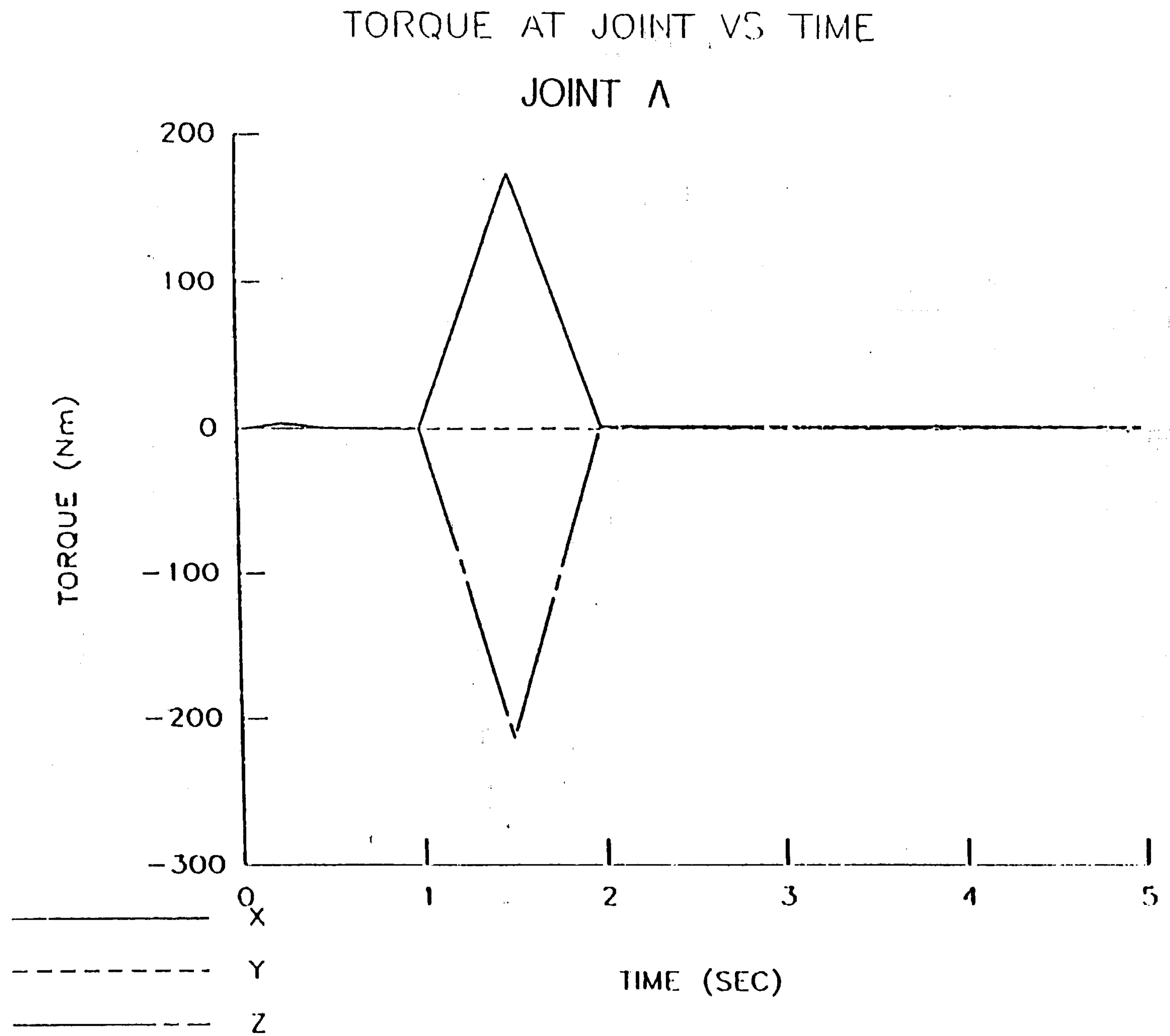
TORQUE AT JOINT VS TIME
JOINT A
TORQUE (Nm)
200
100
0
-100
-200
-300
0
1
2
3
4
5
TIME (SEC)
X
Y
Z

Figure 15

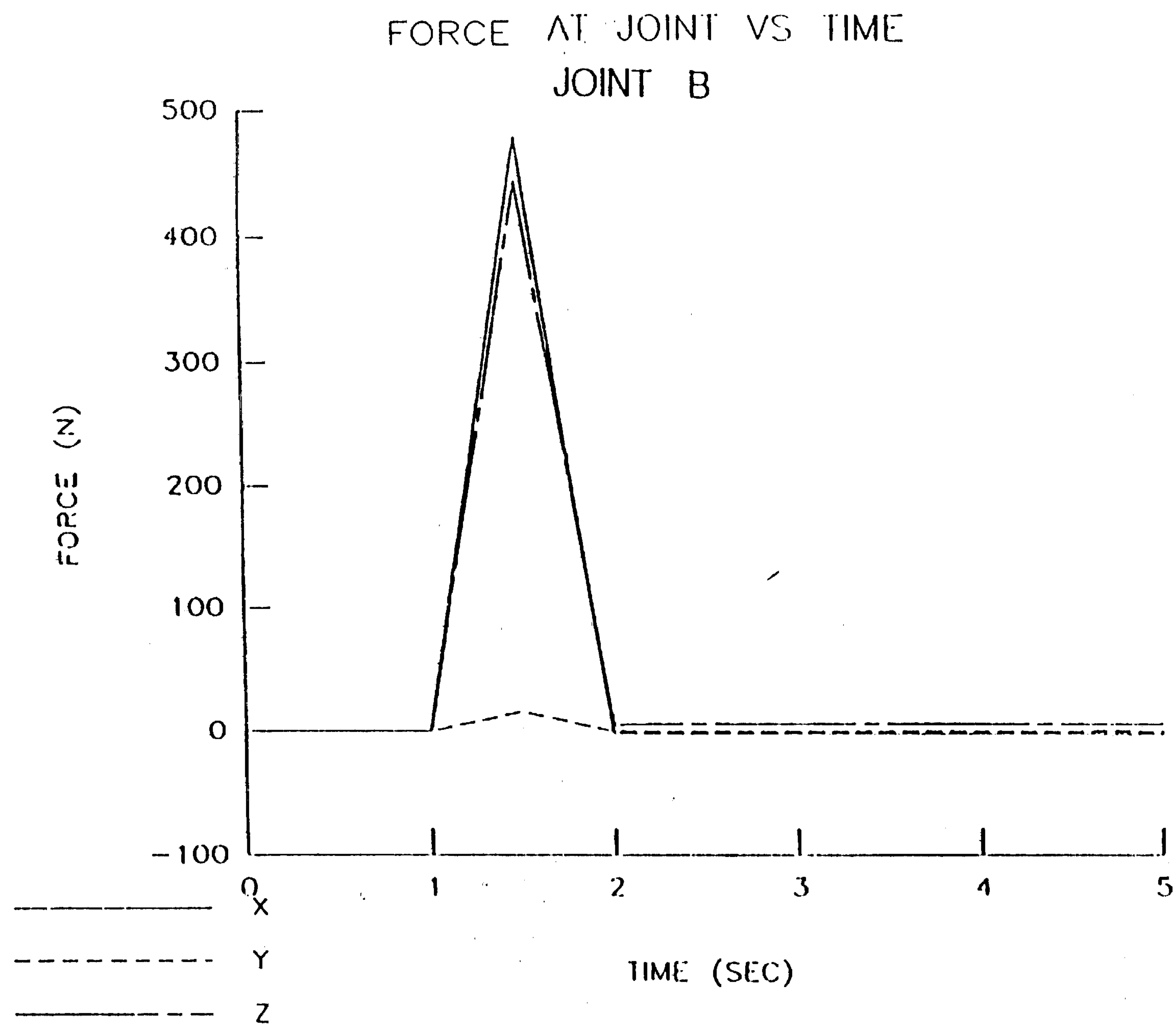

FORCE AT JOINT VS TIME
JOINT B
500
400
300
200
100
0
-100
FORCE (N)
0
1
2
3
4
5
TIME (SEC)
X
Y
Z

Figure 16

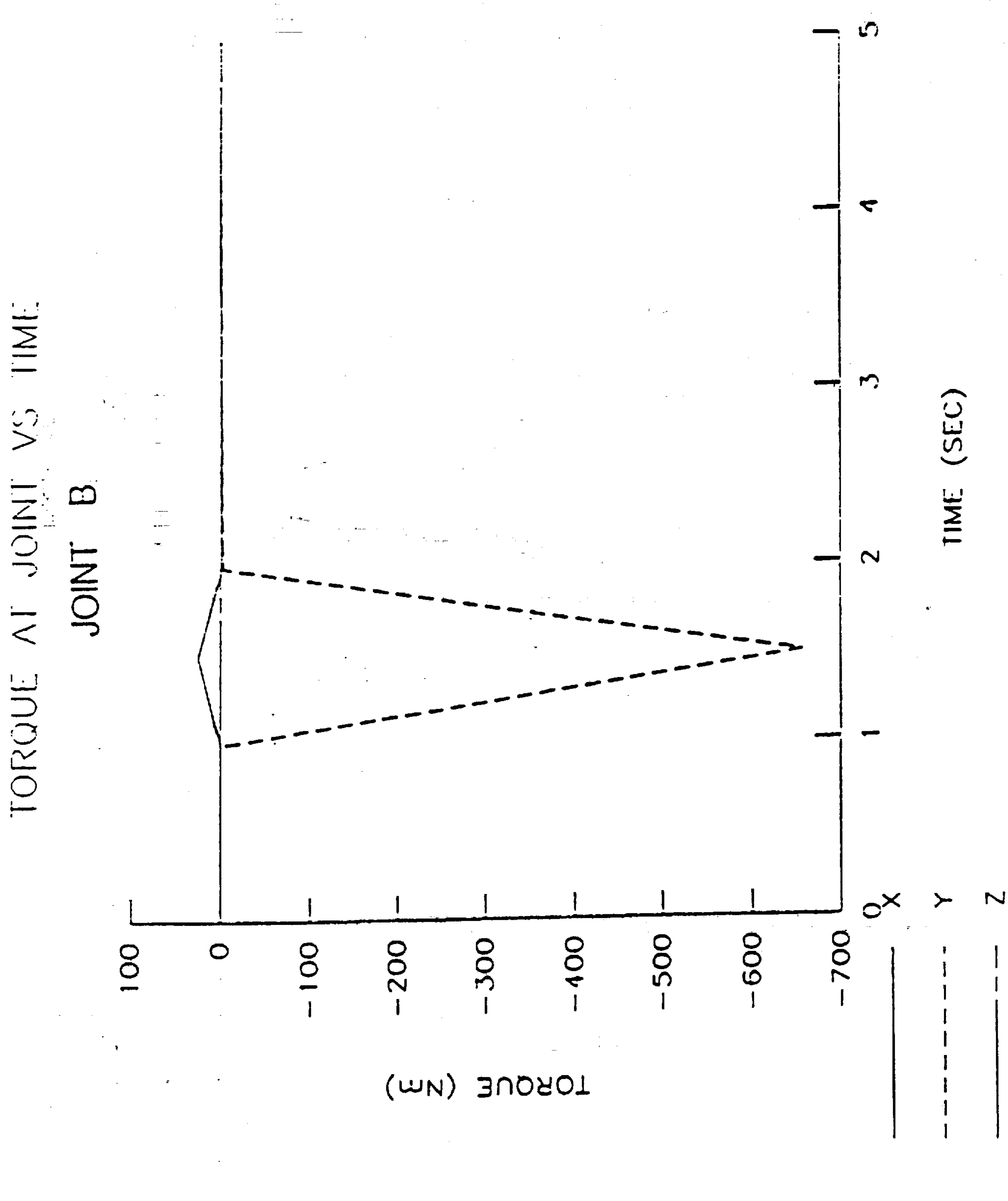
TORQUE AT JOINT VS TIME
JOINT B
TORQUE (Nm)
100
0
-100
-200
-300
-400
-500
-600
-700
0
1
2
3
4
5
TIME (SEC)
X
Y
Z

Figure 17

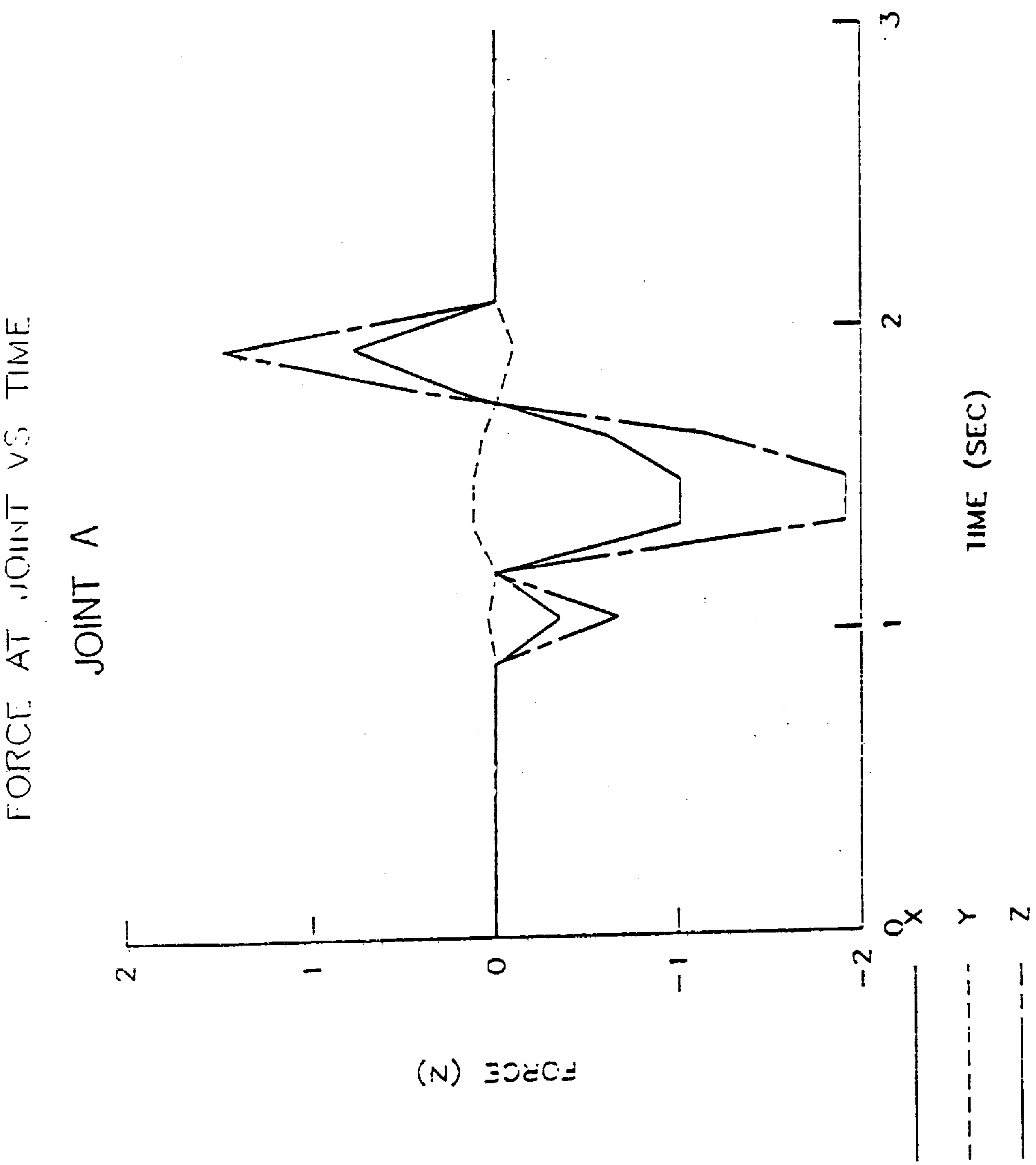

Figure 18

ORIGINAL PAGE IS
OF POOR QUALITY

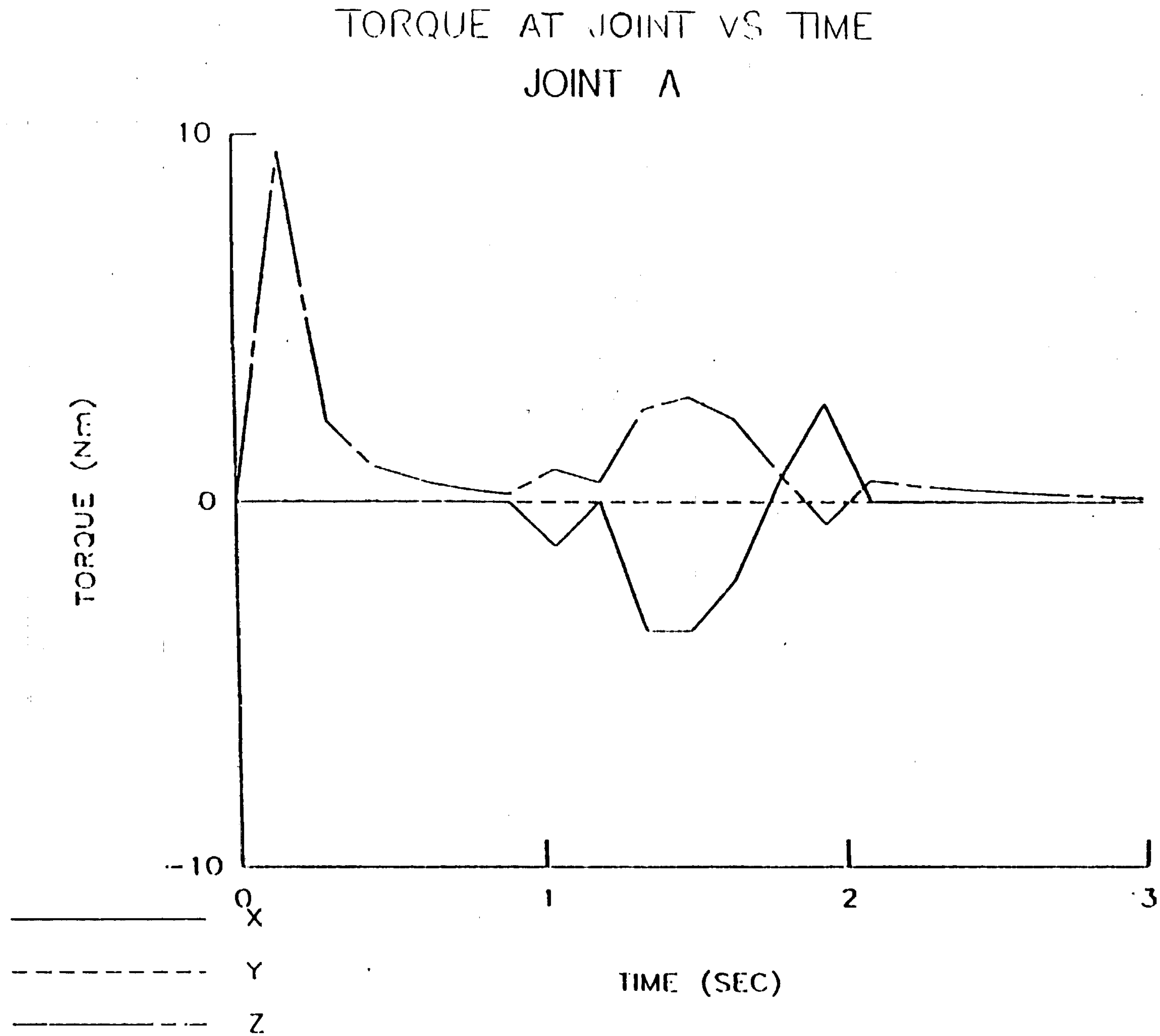
TORQUE AT JOINT VS TIME
JOINT A
10
0
-10
TORQUE (Nm)
0
1
2
3
TIME (SEC)
X
Y
Z

Figure 19

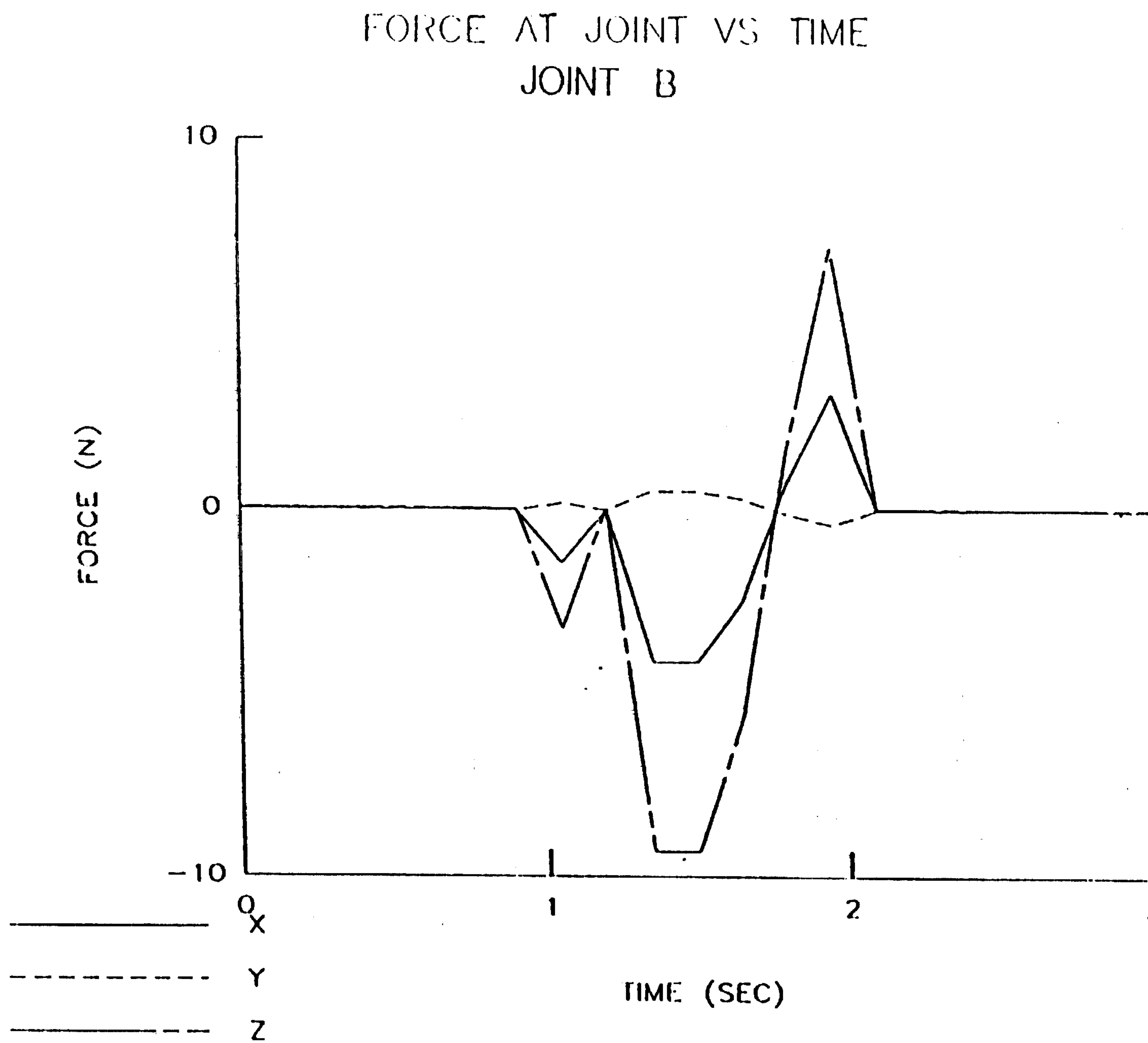

Figure 20

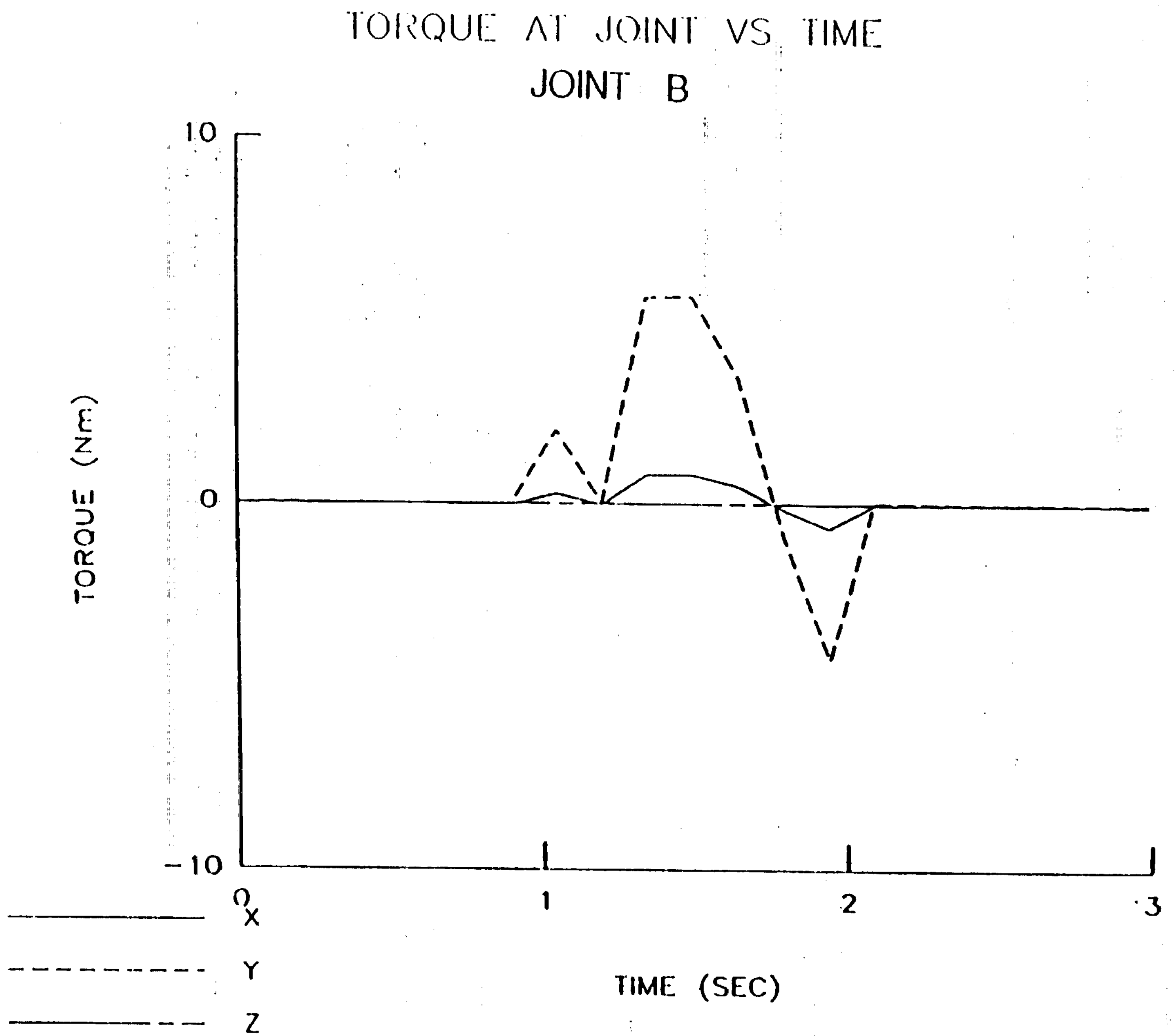
TORQUE AT JOINT VS TIME
JOINT B
10
0
-10
TORQUE (Nm)
0
1
2
3
TIME (SEC)
X
Y
Z

Figure 21

Report Documentation Page

NASA
National Aeronautics and Space Administration

1. Report No. NASA TM-101667	2. Government Accession No.	3. Recipient's Catalog No.
4. Title and Subtitle Dynamic and Control Assessment of the Space Station Freedom Payload Pointing System		5. Report Date February 1991
		6. Performing Organization Code
7. Author(s) David T. Shannon, Jr.		8. Performing Organization Report No.
		10. Work Unit No. 476-14-06-01
9. Performing Organization Name and Address NASA Langley Research Center Hampton, VA 23665-5225		11. Contract or Grant No.
		13. Type of Report and Period Covered Technical Memorandum
12. Sponsoring Agency Name and Address National Aeronautics and Space Administration Washington, DC 20546-0001		14. Sponsoring Agency Code

15. Supplementary Notes

16. Abstract

An analysis of the proposed Space Station Freedom Payload Pointing System (PPS) was performed to assess its dynamic payload pointing capability in the dynamic environment of the Space Station Freedom (SSF). In addition, the stability and control of the Space Station Freedom was examined to verify the capability of its control devices to accommodate the impact of PPS operations. An analysis of the PPS ability to provide continuous, accurate pointing was performed and compared to the program requirements specified in the 1988 Program Definition and Requirements Document (PDRD). Results indicated that the PPS was not able to perform within the program requirements during the worst case scenario of a shuttle hard docking maneuver to the port side SSF docking adapter. The PPS maintained marginal pointing accuracy during crew treadmill activity. The Space Station attitude control system easily accommodated all PPS operations simulated. The PPS caused a negligible impact on Freedom's controls environment.

17. Key Words (Suggested by Author(s)) Space Station Freedom Pointing Capability	18. Distribution Statement Unclassified-Unlimited Subject Category 18

19. Security Classif. (of this report)	20. Security Classif. (of this page)	21. No. of pages	22. Price
Unclassified	Unclassified	34	A03

NASA FORM 1626 OCT 86